Effect of Rare earth substitution on magnetic and structural properties of $Co_{1-x}RE_x Fe_2O_4$ (RE: Nd, Eu) nanoparticles prepared via EDTA/EG assisted sol-gel synthesis

L. Avazpour, H. Shokrollahi, M.R. Toroghinejad, M.A. Zandi Khajeh

PII: S0925-8388(15)31745-X

DOI: 10.1016/j.jallcom.2015.11.188

Reference: JALCOM 36043

To appear in: *Journal of Alloys and Compounds*

Received Date: 5 October 2015

Revised Date: 22 November 2015

Accepted Date: 25 November 2015

Please cite this article as: L. Avazpour, H. Shokrollahi, M.R. Toroghinejad, M.A. Zandi Khajeh, Effect of Rare earth substitution on magnetic and structural properties of $Co_{1-x}RE_x Fe_2O_4$ (RE: Nd, Eu) nanoparticles prepared via EDTA/EG assisted sol-gel synthesis, *Journal of Alloys and Compounds* (2016), doi: 10.1016/j.jallcom.2015.11.188.

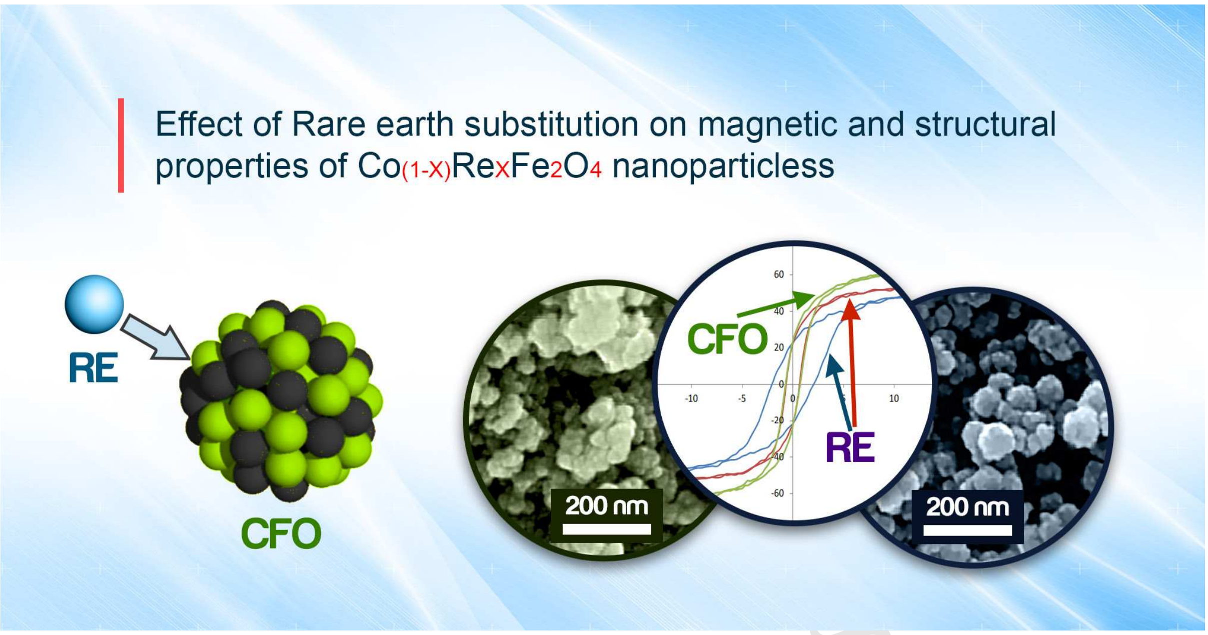

Effect of Rare earth substitution on magnetic and structural properties of $Co_{(1-X)}Re_xFe_2O_4$ nanoparticless

Available online at www.sciencedirect.com
ScienceDirect
00 (2015) 1–12

Effect of Rare earth substitution on magnetic and structural properties of $Co_{1-x}RE_xFe_2O_4$ (RE: Nd, Eu) nanoparticles prepared via EDTA/EG assisted sol-gel synthesis

L. Avazpour[a], H. Shokrollahi [b],M.R.Toroghinejad[a 1],M.A.Zandi Khajeh[b]

[a]Department of Materials Engineering, Isfahan University of Technology, Isfahan
84156-83111, Iran

[b] Electroceramics Group, Department of Materials Science and Engineering, Shiraz University of Technology, Shiraz, Iran

---

Abstract

Four groups of the series of rare earth (RE) substituted cobalt ferrite $Co_{1-x}RE_xFe_2O_4$; x = 0 - 0.2 in steps of 0.05 and RE is Nd and Eu were prepared using the sol-gel method at annealing temperatures 550 °C. The materials were characterized by powder X-ray Diffraction (XRD), Field Emission Scanning Electron Microscopes (FESEM) and Fourier Transform Infrared spectroscopy (FTIR). The phase identification of the materials by XRD reveals the single-phase nature of the materials. The crystallite sizes of the materials were varied by altering the substitution content within the range of a minimum of 11 nm to 31 nm. The magnetic parameters have been studied by using vibrating sample magnetometer (VSM). The saturation magnetization of the ferrite materials at room temperature decreases with the reduction of size. This has been attributed to increased surface to volume ratio and spin canting phenomena. The substituted rare-earth ions inhibit the grain growth of the materials in a systematic manner compared with that of the pure cobalt ferrite materials. There is an improvement in coercivities of the rare earth substituted cobalt ferrite especially for 5 % Neodymium substituted cobalt ferrite with approximately 2 kOe coercive field. This is attributed to the contribution from the single ion anisotropy of the rare-earth ions present in the crystal lattice and the effects of a change in magnetic structures on the surface of the nanoparticles.

Keywords: Cobalt Ferrite, sol-gel, Rare Earth ion, Nanoparticles, Coercive field, Ion substitution.

---

1. Introduction

During last decade, the magnetic nanoparticles, have attracted significant scientific and technological interest because of the wide range of application such as drug-delivery technology [1, 2], liquefied petroleum gas sensing [3] and high-density information storage system [4, 5]. The requirement for these applications will be satisfied by adapting the magnetic properties of these nanoparticles properly. The magnetic properties of these nanoparticles are known to depend dramatically on the physical characteristics such as particle size, chemical composition, cation distribution, surface to volume ratio etc. Among the family of spinel ferrites, particularly cobalt ferrite and substituted cobalt ferrite nanoparticles, have been widely studied due to their interesting properties, which are moderate saturation magnetization, high coercivity, excellent chemical stability, good mechanical hardness and the highest value of magnetostriction, also nanostructured cobalt ferrite exhibits semiconductor behavior from 25-60 °C [6].

We have been interested in carrying out our investigations in order to use cobalt ferrite for high density recording purpose. It has been confirmed that the refinement of the grain size to nanometer content is an effective method for

---

[1] Corresponding author: Email address:toroghi@cc.iut.ac.ir

reducing the noise and increasing signal to noise ratio. Meanwhile, for $CoFe_2O_4$ (CFO) with high Curie temperature 793 K; the cation doping usually needs to be performed in order to increase sensitivity [7]. Rare earth (RE) ions are reported to possess a variety of magnetic properties because of the great variation in the electronic states particularly of the 4f electrons; therefore they are good candidate to tune magnetic properties of CFO [8]. The effect of the Rare earth ion substitution on magnetic properties of the ferrite materials have been examined, especially for using in the applications such as magneto-optical sensors [9], magneto-optical (MO) recording [10] and hyperthermia treatment [11].

Decrease in the Curie temperature T_C and an increase in the effective magnetic moment μ with the increase of Dy^{3+} substitution content on LiCoDy-Ferrites prepared by the standard ceramic technique, was reported; while an anomalous behavior was obtained for the sample with x =0.075 where a rise in T_C and a drop in μ were observed. But the effective sintering temperature was as high as 1200 °C [12]. The influence of the distribution of the metal ions on the magnetic properties of sol-gel derived $CoFe_{2-x}RE_xO_4(0 \leq x \leq 0.03$, RE = Dy, Gd) has been reported by Naik and Salker [13]. Decrease of the particle size and T_B with RE substitution was observed. It was observed that the value of saturation magnetization (M_s) decreases with the RE^+ inclusion that may be correlated with the decrease in particle size brought about with the doping. Amiri and shokrollahi reported the same trend for $Co_{0.9}RE_{0.1}Fe_2O_4$ nanoparticles and thin film, with three different rare earth ions (Nd, Eu, and Gd) prepared by the chemical co-precipitation method [11]. The latter also demonstrated that the coercivity increases by RE doping and reaches its highest content for the Gd^{3+} substituted ferrite at about 914 Oe that is still low for stable magnetic recording media. Also only effect of one substituted contents (x=0.1) was examined. An increase in the surface to volume ratio was evident due to inhabitation of grain growth by RE ions segregation on grain boundaries [11, 12, 13].

The magnetic properties of spinel ferrites are sensitive to the cation distribution between the octahedral and tetrahedral sites [14]. It is evident that due to large radii of rare earth ions, high amount of substitution may result in a drastically cation redistribution of CFO therefore it will have an unwanted impact on magnetic properties hence the doping content x could not exceed more than 0.3. With this in mind we decided to use different doping content to demonstrate best concentration of each rare earth ions for modification of magnetic properties. So in this work we used different contents of dopant to examine and introduce the best concentration of rare earth dopant that will not have unwanted effect on structural and magnetic properties of prepared sample. Therefore, to achieve the homogeneous composition of the final oxide nano-particular powder without any cation segregation, the preparation of a homogeneous gel with respect to the distribution of cations is indispensable. So we used our previous result from our former publication to achieve a homogeneous gel and pure desirable final product [15]. The structural and magnetic properties of the Rare earth-substituted cobalt ferrite nanoparticles prepared by novel EDTA/EG method (reported elsewhere [15]) have been investigated in details.

2. Experimental

All nanoparticles having formula $Co_{1-x}Re_xFe_2O_4$ were prepared by EDTA/EG assisted sol-gel method [15]. Appropriate amount of Ethylene glycol (EG, Sigma-Aldrich), $Fe(NO_3)_3$ (Analytical reagent, Merk.), $Co(NO_3)_2$ (Analytical reagent, Merk.) were dissolved separately in the deionized water by stirring at 70 °C . The adjutant rare earth oxides were dissolved separately in the Nitric acid and deionized water by stirring at 70 °C to obtain RE ions. As ethylenediaminetetraacetic acid (EDTA, Sigma-Aldrich), is insoluble in water, it was dissolved in the concentrated NH_3 at the same temperature. Afterward they were mixed together by stirring for 50 min to obtain a stable and homogenous sol. Then the solution was aged for 2 days. The following step was calcination at 300 °C during 90 min to start decomposition of the resins and result in a black powder. The next step was to anneal the precursor powder at 550 °C for 30 minutes to modify its structure. The steps involved in the synthesis of samples are illustrated in Figure 1.

The heat-treated nano-structured samples were investigated by X-ray diffraction (XRD), thermo gravimetry (TG), Fourier transform infrared spectroscopy (FTIR) and magnetic measurements. The XRD patterns were recorded using a diffractometer (Philips X'pert X-ray Diffractometer) using Cu tube anode (K_α 1.540598). PANalytical X'Pert HighScore software was used for the analysis of different peaks. The field emission scanning electron microscope (FESEM, TESCAN Mira 3-LMU) were employed to study the morphology, particle size and microstructure of the particles. The infrared absorption (IR) spectra of the samples were recorded in the wave number range of 400-4000 cm^{-1} by means of the Perkin Elmer spectrometer using KBr-powder mixed pellets. Magnetic properties of the prepared powder were determined at room temperature using the vibrating sample magnetometer (VSM: Dexing, model 250).

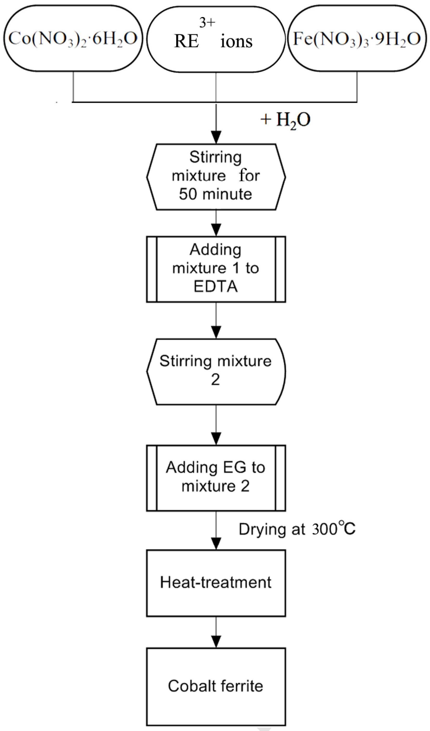

Figure 1. Preparation route for Rare Earth (RE^{3+}) substituted cobalt ferrite nanoparticles by the EDTA/EG precursor method.

3. Results and discussion

3.1. Structural analysis

Mixed spinel ferrites were observed for x =0, 0.05, 0.1, 0.15, 0.2 whereas for x = 0 pure $CoFe_2O_4$ (JCPDS file No: 22-1086) are formed. The formation of rare-earth substituted cobalt ferrites was confirmed by their characteristic powder X-ray diffraction pattern and pattern for 4 samples are shown in Figure 2. All diffraction peaks for the samples correspond to spinel structure with a cubic structure. The X-ray diffraction patterns do not contain any extra reflection corresponding to oxides of Nd, Eu or Fe.

X-ray diffraction and differential thermal analysis measurements for Co ferrite powders show crystallization temperatures of the ferrite powders are about 350 °C, however, the formation of a magnetically and structurally homogeneous ferrite sample requires the annealing temperature above 550 °C. The patterns also show a slight shift in peaks position towards higher d-spacing. The peaks become broader toward higher rare earth ions substitution content which is significant of finer particles. The broadening of the peaks also accommodated with the decrease in the density due to an increase in the surface to volume ratio of the compounds with the doping of RE^{3+} ions. The growth of the crystalline grains is also restricted by the substituting of rare earth ions, leading to the relative small grains. It is observed that lattice constant is increased linearly by increasing substitution content. The reason for this increase in lattice parameter values may be due to the larger ionic radii of RE^{3+} as compared to Co^{3+} .The crystallite size has been calculated using Scherrer's formula.

$$D = \frac{k\lambda}{\beta \cos\theta} \tag{1}$$

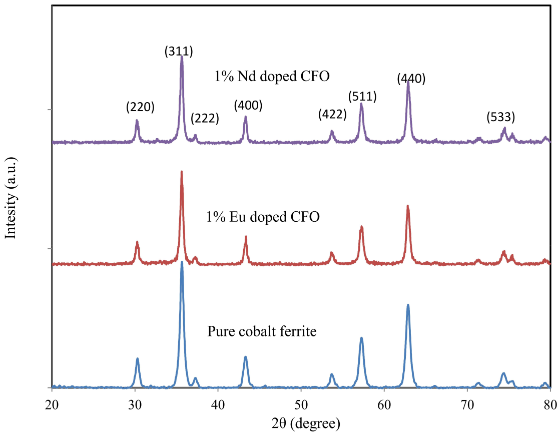

Figure 2. X-ray diffraction pattern of $CoFe_2O_4$; $Co_{0.9}Eu_{0.1}Fe_2O_4$; $Co_{0.9}Nd_{0.1}Fe_2O_4$; heat-treated at 550 °C. The absence of any impurity phase is visible.

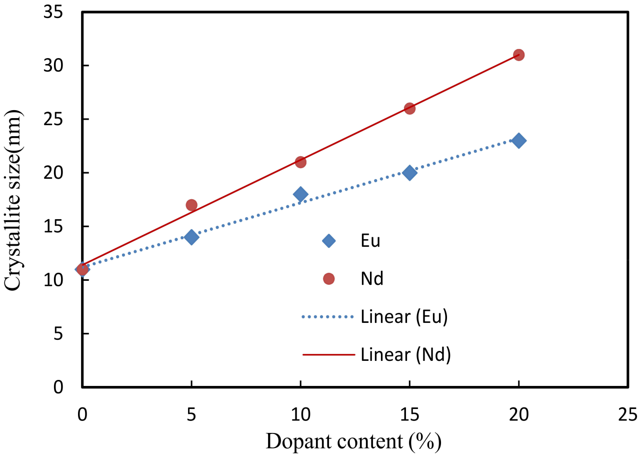

Figure 3. The calculated crystallite sizes vs. doping content of samples

Where the constant k depends upon the shape of the crystallite size (which is equivalent to 0.89, assuming the circular grain), β is the full width at half maximum of the intensity (a.u.) vs. 2θ profile, λ is the wavelength of the CuK_α radiation (equal to 0.1542 nm), θ is the Bragg's diffraction angle, and D is the crystallite size. In Scherrer's formula, the average crystallite size has been calculated using the Gaussian fit, fitted to the highest peak in the XRD pattern (within an error of 2 nm). The calculated crystallite sizes versus doping content of samples are shown in Figure 3. As the electron orbital tend to be completed or half completed the interaction tendency with environmental anions decreases and consequently the crystallite size and the particle size decreases [16]; Therefore for substitution of Eu ($6s^2 4f^7$) we have smaller crystallite size than for substitution of Nd ($6s^2 4f^4$) in cobalt ferrite crystal lattice As shown in Figure 3. From FESEM image of pristine and RE substituted cobalt ferrite it can be seen that the RE substituted nanoparticles are less agglomerated; the RE^{3+} ions will segregate close to the grain boundaries thereby minimizing the possibility of increasing the grain size due to the agglomeration process [17, 18]. The average particle sizes were determined from the FESEM image; Pristine Cobalt ferrite has the average particle size of 33 nm and for 20 % Eu substituted CFO it was 23 nm (Figure 4.) and the later shows narrow particle size distribution. The dislocation density (δ), defined as the length of dislocation per unit volume, which gives the number of defects in a crystal, was estimated. The dislocation density (δ) was calculated with the following relation [19]:

$$\delta = 1/D^2_{avg} \tag{2}$$

Where D_{avg} is the average crystallite size. Lower values of the dislocation density indicate good crystallinity of the prepared samples. The results are shown in table 1.

3.2. FTIR analysis

FTIR spectra of pristine cobalt ferrite and Eu substituted cobalt ferrite ($Co_{1-x}Eu_xFe_2O_4$) ; x=0.05,0.1 heat-treated at 550 °C and the aged gel of cobalt ferrite are shown in Figure 5. In spectra of aged gel there exists some broadband absorption peak due to the stretching vibration of precursors such as peak at 3284 cm^{-1} due to the N − H stretching vibration. As the Annealing temperature increases to 550 °C, the absorption bands of frequencies higher than 1000 cm^{-1} disappeared. The absence of the peaks at 1000-1300 cm^{-1} and 2000-3000 cm^{-1} in the samples Annealed at 550 °C confirms the nonexistence of the O − H mode, C − O mode, and C = H stretching mode of the organic sources. Hence, there are no residual organic compounds.

Two prominent peaks centered at 583 cm^{-1} (ν1) and 407 cm^{-1} (ν2) represent metal-oxygen bond stretching in the tetrahedral and octahedral lattices. The observed absorption pattern reveals the formation of the spinel lattice. The tetrahedral peak in the FTIR spectra positions at a higher region as compared to that of the octahedral peak. The metal-oxygen bond in the tetrahedral lattice has a shorter bond length as compared to that in the octahedral lattice and therefore more energy is required to vibrate the bond. It is known that increasing site radius reduces the fundamental frequency and therefore the peak frequency should shift towards the lower frequency side. It can be seen from the figure that as the substitution content of RE^{3+} is increasing, the intensity of the bands at 579 cm^{-1} increases and shifts towards higher frequency. The high frequency band becomes broad and the band at 407 cm^{-1} is shifted to lower frequency when the percent of Rare earth ion dopant is increasing. This indicates that RE^{3+} Ions occupy octahedral sites of spinel structure. The structural parameters of octahedral and tetrahedral sites and the interatomic bond lengths for 5 samples are listed in tables 2 and 3.

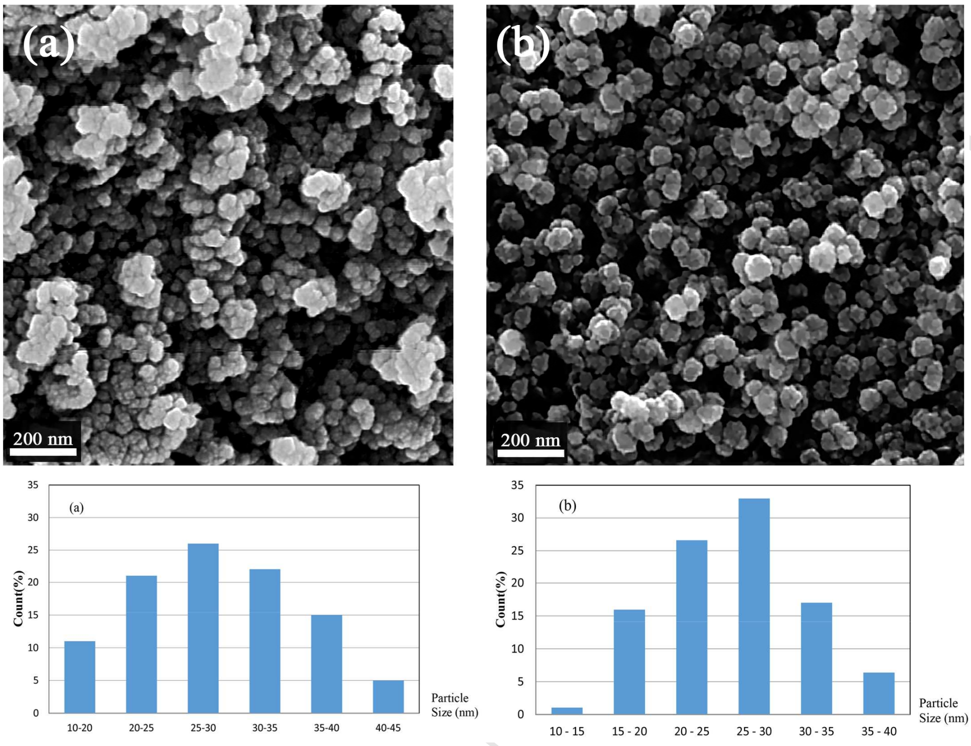

Figure 4. FESEM image of (a) $CoFe_2O_4$ (b) $Co_{0.9}Eu_{0.1}Fe_2O_4$

3.3. Magnetic Behaviour

The magnetization of the prepared samples was characterized with a VSM. Figure 6 shows the room temperature magnetic hysteresis loops of nanocrystalline Pristine cobalt ferrite (CFO), 5% Eu substituted cobalt ferrite $Co_{0.95}Eu_{0.05}Fe_2O_4$: E1 and 5% Nd substituted cobalt ferrite $Co_{0.95}Nd_{0.05}Fe_2O_4$: N1, heat-treated at 550 °C. The maximum applied magnetic field in the instrument was 15 kOe. It shows the semi-hard ferrimagnetic nature (i.e. higher coercivity compared to soft magnets) of the samples synthesized by the EDTA/EG assisted sol-gel process. The magnetic behavior, such as saturation magnetization (M_s), coercivity (H_c), remanent magnetization (M_r), and squareness ratio (SQR) obtained from the M-H loops are listed in table 1.

3.3.1. Saturation magnetization

In general, magnetic properties of nanoparticles depend on the synthesis conditions, particle size and the cation distribution among the different sites. Saturation magnetization of obtained CFO is lower than theoretical M_s of CFO or bulk CFO (80 emu/g) [20] due to spin canting effect at the surface of nanoparticles that reduces overall magnetization of nanoparticle samples. After the doping, the observed M_s decreases from 59.2 to 44.3 emu/g with increase in the dopant content. Due to the unfilled 4f shells of rare-earth atoms, it is a challenging problem to obtain

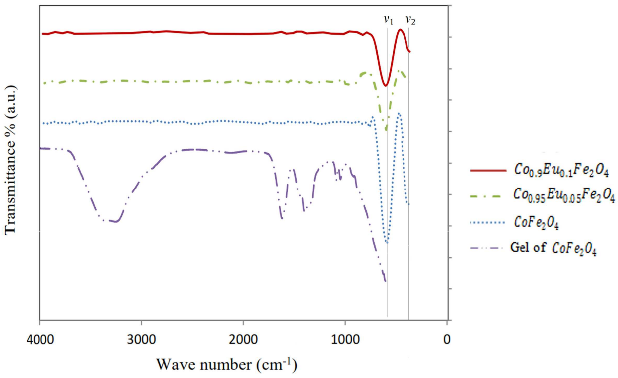

Figure 5. The FTIR spectra of the aged gel; Pristine cobalt ferrite and Eu substituted cobalt ferrite ($Co_{1-x}Eu_xFe_2O_4$), x=0.05, 0.1 heat-treated at 550 °C

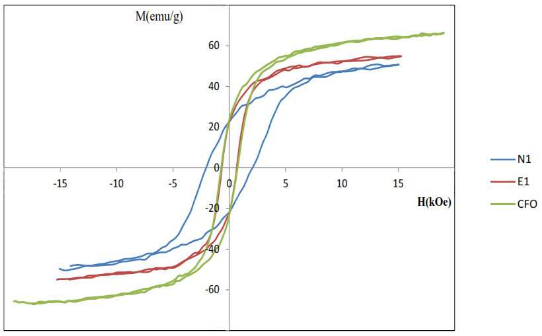

Figure 6. M-H loops at room temperature for Pristine cobalt ferrite (CFO), 5% Eu substituted cobalt ferrite $Co_{0.95}Eu_{0.05}Fe_2O_4$: E1 and 5% Nd substituted cobalt ferrite $Co_{0.95}Nd_{0.05}Fe_2O_4$: N1, heat-treated at 550° C

an accurate theoretical description of the electronic structure of rare-earth compounds. In spite of the fact that the 4f energy contents often overlap with the non-4f broad bands of the system, they generally form very narrow resonances, and are often treated as core states in the theoretical efforts. Due to the highly localized nature of the 4f electrons, the direct f-f interactions between neighboring rare-earth atoms are generally considered to be nearly negligible.

As we know $CoFe_2O_4$ normally has an inverse-spinel structure, where Co^{2+} ions occupy octahedral sites, while Fe^{3+} ions occupy both tetrahedral and octahedral lattice sites [6]. The substitution of Co with RE ions takes place at octahedral sites due to their larger ionic radii. Hence it is expected that the number of magnetic moments on the octahedral site decrease. Therefore, the magnetic moment of B-sublattice decreases and consequently magnetization also decreases. It can be explained by the fact that by introducing RE^{3+} to CFO lattice the number of magnetic linkages occurring between tetrahedral and octahedral cations is decreasing. The RE^{3+} -Fe^{3+} interaction (4f-3d coupling) and the RE^{3+} -RE^{3+} interaction (indirect 4f-5d-4f electrons coupling) exist but they are very weak. The A-B interaction heavily predominates over A-A and B-B interactions [21].

Spin ordering in RE doped CFO is ferrimagnetic; includes unbalanced antiparallel spins. As a general rule, any electrically insulating compound containing only rare-earth ions, with the exceptions of Eu^{2+}, will have extremely weak exchange interactions. This is because the 4f contents in the trivalens rare earths lie deep within the ion. In case of Eu calgogenides the 4f contents are only 1-2 eV below the outer valence electrons, and the wave functions of the 4f electrons overlap adjacent ions is much stronger. The third valence electron Eu^{2+} to Eu^{3+} is easily promoted into a virtual 5d state which acts to enhance the exchange interaction in low concentration.[22]. Hence as we see from figure 6, the saturation magnetization of Eu^{3+} substituted CFO are slightly higher than Nd^{3+} doped compound but both have descending trend compared to pristine CFO. The saturation magnetizations of samples are higher than reported M_s of previous Neodymium doped CFO that was prepared via sol-gel method [23]. This can be related to absence of hematite phase as one of the frequently formed impurity phase in ferrites in current samples. In previous works despite the 4 hours sintering, presence of hematite phase was detected [23, 24].

In spinel lattice total magnetic moment is $M_{oct} - M_{tet}$(M_{oct} and M_{tet} are the sum of the magnetic moments on B sites and A sites, respectively). As it is seen from Figure 7, overall trend of Ms of substituted samples is descending by increasing dopant content. But there exists a slight increase for Eu content of 5% and 10% . The increment of the saturation magnetization at Eu content (x = 0.05, 0.1) can be explained by the fact that the substitution of Eu ions by Co ions in octahedral sites increases the magnetization as the magnetic moments of Eu^{2+} and Co^{2+} are 7.9 and 3 μ_B, respectively. However, with further increase in the Eu concentration (x = 0.15 and 0.2), the magnetization instantly decreases because the conversion of equivalent amounts of Fe^{3+} ($5\mu_B$) to Fe^{2+} ($4\mu_B$) [25]. Also by increasing dopant content particle size of the sample will decrease as a result due to dominant spin canting effect for particles less than about 15 nm we see by reduction of size there is a decrease in saturation magnetization.

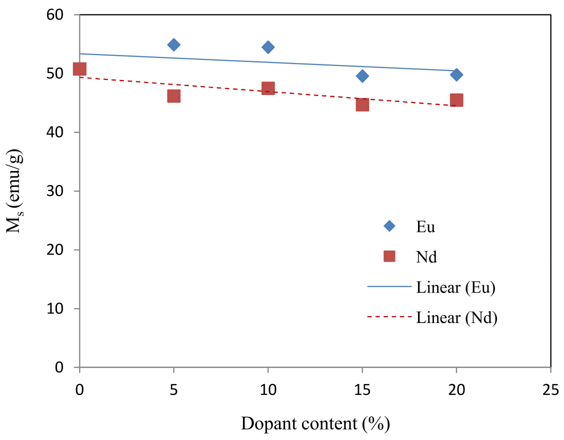

Figure 7. Saturation magnetization of Eu and Nd substituted cobalt ferrite vs. dopant content

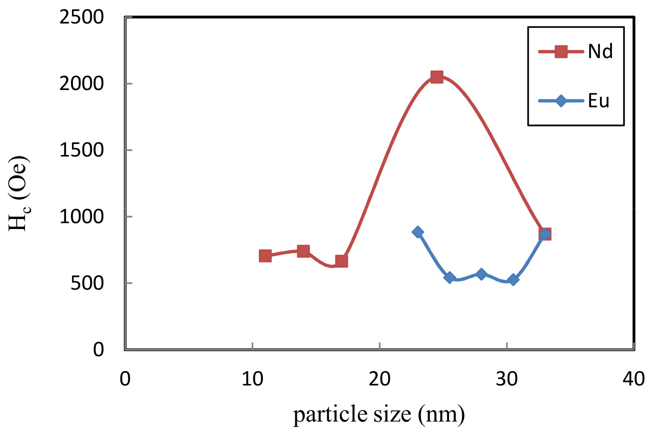

Figure 8. Coercivity vs. particle size of Nd and Eu substituted cobalt ferrite with different doping content

3.3.2. Coercivity

The coercivity H_c which measures the magnetic field strength required for overcoming anisotropy to flip the magnetic moments is clearly affected by the RE substitution. The value of coercivity (H_c), reaches a maximum value and then decreases as the grain size increases. Highest coercivity is observed for 5% Nd substituted CFO. It is reported that coercivity depends on factors such as magneto-crystalline anisotropy, microstrain, size distribution, anisotropy and the magnetic domain size [26, 27].The target crystal size is within the superparamagnetic and single domain limits region (5-70nm), in which case H_c can be possibly improved [28, 29, 30]. The increase in coercivity with an increase in particle size at room temperature in the single-domain region can be explained by use of Kramers treatment and in multi-domain region there is increase in coercivity with decrease in particle size [31]. As the particle size of obtained samples are within single-domain particle size limit we observe an increase in coercivity with decrease of particle size to a critical diameter for 5% Neodymium doped cobalt ferrite. After that there is a decrease in coercivity of samples as shown in Figure 8. So the optimum hard magnetic properties arise due to the formation of single domain particles. The coercivity of sample reaches its highest level for x=0.05 and Nd^{3+} as doping ion. This increase can be explained as follows:

i) The RE^{3+} ions known to have strong spin-orbit coupling and promote the asymmetrical structure of the nanoparticles as they are located at the B sites [32]. In high content doping the effect of the single ion anisotropy of RE^{3+} is rather small as compared to the cation rearrangement caused by introduction of large radius of these ions in CFO crystal lattice. Because the 4f shell of the RE ions is shielded by the 5s and 5p electrons, the crystal field perturbation are small so no orbital quenching occurs [8]. The doping with 5% magnetic Nd^{3+} ions increases the coercive force of cobalt ferrite due to the contribution of their large single ion anisotropy.

ii) Another reason for this huge improvement in coercivity can be attributed to the domain wall pinning. Therefore, the magnetic coupling at the individual lattice sites lead to this phenomenon that movement of the magnetic domain wall will become more difficult and a relatively large coercive force is anticipated for the present $Co_{0.95}Nd_{0.05}Fe_2O_4$ nanocrystalline sample. But for higher content of Nd ions along with the reduction of crystallite size, the particle size also decreases; this leads to formation of single domain per particles (as the particles are not all the same size we don't have perfect superparamagnet) as a result the coercive field of doped cobalt ferrite decreases. This consideration came from the reported formation of single domain inside each grain of nano grain ferrites. Furthermore, the decrease in the coercivity for the high amounts of RE is related to the noticeable replacement of Co^{2+} by Nd^{3+} and cation rearrangement.

The mechanism by which magnetization reversal occurs involves several events which are inherently linked to the presence of defects. These events, nucleation, propagation and pinning-depinning of a domain wall, are strongly linked to the microstructure [33]. With an increase in the nano crystallite size the sample becomes more homogenous as some intra pores drift to the grain boundaries. So the decrease of the defects concentrations (intra pores) inside the grains will occur; As a result the coercivity of 5, 10 and 15% Eu doped sample decreases. But by further increase of Eu content the dominant factor for the increase of Hc will be the increase of inter granular pores for single domain nanocrystalline because as can be seen from XRD result and FESEM the 20% Eu doped sample appears to be mostly single domain single grain nanoparticles.

A decrease in T_C by increasing RE ion content is observed. The moments of f orbital generally cannot be quenched by the crystal field. Therefore the total magnetic moments have both orbital and spin components, and spin-orbital interactions are particularly strong for many of the rare-earth mediated compounds. These inner shell magnetic moments are largely aligned through intra-atomic s(d)-f exchange interaction and weaker inter-atomic s-s (d-d) exchange interactions; thus the rare earth substituted cobalt ferrite magnetic transition temperatures are generally much lower than those of cobalt ferrite.

4. Conclusion

A simple sol-gel process based on EDTA/EG-nitrate has been used to demonstrate the effect of neodymium and europium ions substitution on structure and magnetic properties of $CoFe_2O_4$. The RE doped CFO nanoparticles can be produced in large quantity with size ranging from the threshold of 10 nm to 40 nm. The phase analysis of the samples showed that the structure of the single phase products was obtained. From the cation distribution studies, it can be concluded that these RE ions substitute Co ions in the octahedral sites probably due to their ionic radius which is close to the limiting size of the octahedral sites. By introducing more than 10 % RE ions to the crystal structure probability of occurrence of the Fe_2O_3 impurity phase is increasing. This reflects the limiting capacity of the lattice to incorporate RE ions in its crystal structure. With the increase of content of the rare earth ions the average crystallite size increases due to larger ionic radii of RE ions compared to Co ions and average particle size decreases that can be related to octahedral site preference of RE ions which causes a main part of energy to be consumed to the cations internal displacement or configurational entropy instead of grain growth. With the synthesis method reported here heat-treatment at 550 °C for 30 minutes was enough to obtain the pure samples with an appropriate structure for their composition. It is observed that coercivity of sample with $Co_{0.95}Nd_{0.05}Fe_2O_4$ composition reaches to maximum of 2 kOe. The optimum hard magnetic properties of rare earth doped cobalt ferrite arise due to the formation of single domain particles. Thus we can tune the magnetic properties of the cobalt ferrite nanoparticles by appropriate choice of the neodymium or europium ion concentration and make it suitable for technological applications.

References

[1] T. Tetsushi, A. Takao, From biomedical-engineering research to clinical application and industrialization, Science and Technology of Advanced Materials, 13 (2012) 060301.

[2] T.J. Yoon, J.S. Kim, B.G. Kim, K.N. Yu, M.H. Cho, J.K. Lee, Multifunctional nanoparticles possessing a magnetic motor effect for drug or gene delivery, Angewandte Chemie, 117 (2005) 1092-1095.

[3] S. Singh, A. Singh, B.C. Yadav, P. Tandon, Synthesis, characterization, magnetic measurements and liquefied petroleum gas sensing properties of nanostructured cobalt ferrite and ferric oxide, Materials Science in Semiconductor Processing, 23 (2014) 122-135.

[4] S. Dabagh, A.A. Ati, R.M. Rosnan, S. Zare, Z. Othaman, Effect of Cu-Al substitution on the structural and magnetic properties of Co ferrites, Materials Science in Semiconductor Processing, 33 (2015) 1-8.

[5] L. Wang, C.-H. Yang, S. Gai, J. Wen, Current Status and Future Prospects of Conventional Recording Technologies for Mass Storage Applications, Current Nanoscience, 10 (2014) 638-659.

[6] R. Atta ur, M.A. Rafiq, S. Karim, K. Maaz, M. Siddique, M.M. Hasan, Semiconductor to metallic transition and polaron conduction in nanostructured cobalt ferrite, Journal of Physics D: Applied Physics, 44 (2011) 165404.

[7] I. Sharifi, H. Shokrollahi, Nanostructural, magnetic and Mssbauer studies of nanosized $Co_{1-x}Zn_xFe_2O_4$ synthesized by co-precipitation, Journal of Magnetism and Magnetic Materials, 324 (2012) 2397-2403.

[8] J. JENSEN, A.R. MACKINTOSH, Rare Earth Magnetism Structures and Excitations, CLARENDON PRESS, OXFORD, 1991.

[9] Y. Mohammadifar, H. Shokrollahi, Z. Karimi, L. Karimi, The synthesis of $Co_{1-x}Dy_xFe_2O_4$ nanoparticles and thin films as well as investigating their magnetic and magneto-optical properties, Journal of Magnetism and Magnetic Materials, 366 (2014) 44-49.

[10] B. Zhou, Y.-W. Zhang, C.-S. Liao, C.-H. Yan, L.-Y. Chen, S.-Y. Wang, Rare-earth-mediated magnetism and magneto-optical Kerr effects in nanocrystalline $CoFeMn_{0.9}RE_{0.1}O_4$ thin films, Journal of Magnetism and Magnetic Materials, 280 (2004) 327-333.

[11] S. Amiri, H. Shokrollahi, Magnetic and structural properties of RE doped Co-ferrite (RE:Nd, Eu, and Gd) nano-particles synthesized by co-precipitation, Journal of Magnetism and Magnetic Materials, 345 (2013) 18-23.

[12] M.A. Ahmed, S.T. Bishay, The role of Dy^{3+} ions and sintering temperature on the magnetic characterization of LiCo-Ferrite, Journal of Magnetism and Magnetic Materials, 279 (2004) 178-183.

[13] S. Naik, A. Salker, Change in the magnetostructural properties of rare earth doped cobalt ferrites relative to the magnetic anisotropy, Journal of Materials Chemistry, 22 (2012) 2740-2750.

[14] D. Carta, M. Casula, A. Falqui, D. Loche, G. Mountjoy, C. Sangregorio, A. Corrias, A structural and magnetic investigation of the inversion degree in ferrite nanocrystals MFe_2O_4 (M= Mn, Co, Ni), The Journal of Physical Chemistry C, 113 (2009) 8606-8615.

[15] L. Avazpour, M.A. Zandi khajeh, M.R. Toroghinejad, H. Shokrollahi, Synthesis of single-phase cobalt ferrite nanoparticles via a novel EDTA/EG precursor-based route and their magnetic properties, Journal of Alloys and Compounds, 637 (2015) 497-503.

[16] R. Arulmurugan, G. Vaidyanathan, S. Sendhilnathan, B. Jeyadevan, Mn-Zn ferrite nanoparticles for ferrofluid preparation: Study on thermal-magnetic properties, Journal of Magnetism and Magnetic Materials, 298 (2006) 83-94.

[17] J. Feng, Li-Qin Guo, X. Xu, S.Y. Qi, Mi-Lin Zhang, Hydrothermal synthesis and characterization of $Mn_{1-x}Zn_xFe_2O_4$ nanoparticles, Physica B: Condensed Matter, 394 (2007) 100-103.

[18] J. Wang, C. Zeng, Z.M. Peng, Q.W. Chen, Synthesis and magnetic properties of $Zn_{1-x}Mn_xFe_2O_4$ nanoparticles, Physica B: Condensed Matter, 349 (2004) 124-128.

[19] P. Kathirvel, D. Manoharan, S.M. Mohan, S. Kumar, Spectral Investigations of Chemical Bath Deposited Zinc Oxide Thin Films - Ammonia Gas Sensor Journal of Optoelectronic and Biomedical Materials, 1 (2009) 25-33.

[20] T. George, A.T. Sunny, T. Varghese, Magnetic properties of cobalt ferrite nanoparticles synthesized by sol-gel method, IOP Conference Series: Materials Science and Engineering, 73 (2015) 012050.

[21] I. Ali, M. Islam, M. Ishaque, H.M. Khan, M.N. Ashiq, M. Rana, Structural and magnetic properties of holmium substituted cobalt ferrites synthesized by chemical co-precipitation method, Journal of Magnetism and Magnetic Materials, 324 (2012) 3773-3777.

[22] J.J. Rhyne, T.R. McGuire, Magnetism of rare-earth elements, alloys, and compounds, Magnetics, IEEE Transactions on, 8 (1972) 105-130.

[23] S. Xavier, S. Thankachan, B. Jacob, E. Mohammed, Effect of Neodymium Substitution on Structural and Magnetic Properties of Cobalt Ferrite Nanoparticles. J Nanomater Mol Nanotechnol 2: 7, of, 6 (2013) 2.

[24] S. Thankachan, B.P. Jacob, S. Xavier, E. Mohammed, Effect of neodymium substitution on structural and magnetic properties of magnesium ferrite nanoparticles, Physica Scripta, 87 (2013) 025701.

[25] T. Moeller, Advances in Inorganic Chemistry and Radiochemistry, Journal of the American Chemical Society, 83 (1961) 1520-1520.

[26] B.D. Cullity, C.D. Graham, Introduction to magnetic materials, John Wiley & Sons2011.

[27] C. Suvankar, B. Malay, Coercivity of magnetic nanoparticles: a stochastic model, Journal of Physics: Condensed Matter, 19 (2007) 216201.

[28] S. Goh, C. Chia, S. Zakaria, M. Yusoff, C. Haw, S. Ahmadi, N.M. Huang, H.N. Lim, Hydrothermal preparation of high saturation magnetization and coercivity cobalt ferrite nanocrystals without subsequent calcination, Materials Chemistry and Physics, 120 (2010) 31-35.

[29] G.C. Papaefthymiou, Nanoparticle magnetism, Nano Today, 4 (2009) 438-447.

[30] K.J. Buschow, Concise encyclopedia of magnetic and superconducting materials, Elsevier, 2005.

[31] S. Chakraverty, M. Bandyopadhyay, Coercivity of magnetic nanoparticles: a stochastic model, Journal of Physics: Condensed Matter, 19 (2007) 216201.

[32] F.X. Cheng, J.T. Jia, Z.G. Xu, B. Zhou, C.S. Liao, C.H. Yan, L.Y. Chen, H.B. Zhao, Microstructure, magnetic, and magneto-optical properties of chemical synthesized CoRE (RE= Ho, Er, Tm, Yb, Lu) ferrite nanocrystalline films, Journal of applied physics, 86 (1999) 2727-2732.

[33] D. Givord, M. Rossignol, D. Taylor., Coercivity mechanisms in hard magnetic mater

Table 1. Crystallite size,saturation magnetization , Coercive field, dislocation density, lattice parameter and squareness of samples heat treated at 550 °C

Sample name	Sample composition	D_{avg} (nm)	M_s (emu/g)	H_c(Oe)	δ	lattice parameter (Å)	SQR
CFO	$CoFe_2O_4$	11	50.8	869	0.0021	8.347	0.36
E1	$Co_{0.95}Eu_{0.05}Fe_2O_4$	14	54.9	527	0.0025	8.348	0.52
E2	$Co_{0.90}Eu_{0.10}Fe_2O_4$	18	54.5	568	0.0030	8.348	0.41
E3	$Co_{0.85}Eu_{0.15}Fe_2O_4$	20	49.6	543	0.0038	8.350	0.37
E4	$Co_{0.80}Eu_{0.20}Fe_2O_4$	23	49.8	885	0.0051	8.351	0.37
N1	$Co_{0.95}Nd_{0.05}Fe_2O_4$	17	46.2	2050	0.0023	8.354	0.40
N2	$Co_{0.90}Nd_{0.10}Fe_2O_4$	21	47.5	665	0.0025	8.365	0.36
N3	$Co_{0.85}Nd_{0.15}Fe_2O_4$	26	44.7	740	0.0033	8.373	0.32
N4	$Co_{0.80}Nd_{0.20}Fe_2O_4$	31	45.5	706	0.0035	8.382	0.40

Table 2. Structural parameters of octahedral and tetrahedral sites

Sample name	Dopant ion	Dopant content	r_A (nm) Tetrahedral Coordination	r_B (nm) Octahedral Coordination	lattice parameter (Å)
CFO	-	0.00	0.7086	0.7374	8.347
N1	Nd	0.05	0.7103	0.7391	8.354
N2	Nd	0.10	0.7057	0.7344	8.365
E2	Eu	0.10	0.7065	0.7352	8.348
E3	Eu	0.15	0.7069	0.7356	8.350

Table 3. Interatomic bond lengths

$M_e - O$(Å)					$M_e - M_e$(Å)				
	p	q	r	s	b	c	d	e	f
CFO	0.0952	0.3769	0.7225	0.4265	0.2942	0.3460	0.3610	0.5415	0.5112
N1	0.0954	0.3777	0.7241	0.4274	0.2949	0.3468	0.3618	0.5426	0.5123
N2	0.0951	0.3768	0.7224	0.4264	0.2942	0.3460	0.3609	0.5414	0.5111
E2	0.0952	0.3769	0.7226	0.4265	0.2943	0.3461	0.3611	0.5416	0.5113
E3	0.0952	0.3770	0.7228	0.4266	0.2943	0.3462	0.3611	0.5417	0.5114

Research Highlights

- Nanostructured rare earth doped Co-ferrite particles were synthesized by sol-gel.
- The coercivity of as high as 2 kOe is achieved for 5% substituted cobalt ferrite.
- The saturation magnetization is decreasing by increasing Nd^{3+} substitution content.
- Obtained nanoparticles are single-domain particles.